



CLIMADAT-GRid: A high-resolution daily gridded precipitation and temperature dataset for Greece

Konstantinos V. Varotsos¹, Gianna Kitsara¹, Anna Karali¹, Ioannis Lemesios¹, Platon Patlakas², Maria Hatzaki³, Vassilis Tenentes¹, George Katavoutas¹, Athanasios Sarantopoulos⁴, Basil Psiloglou¹

5 Aristeidis G. Koutroulis⁵, Manolis G. Grillakis⁵, Christos Giannakopoulos¹

¹Institute for Environmental Research and Sustainable Development, National Observatory of Athens, Athens, 15236, Greece

²Department of Physics, National and Kapodistrian University of Athens, Athens, 15784, Greece

10 ³Laboratory of Climatology and Atmospheric Environment, Section of Geography and Climatology, Department of Geology and Geoenvironment, National and Kapodistrian University of Athens, Athens, 15784, Greece

⁴Hellenic National Meteorological Service, Athens, 16777, Greece

⁵School of Chemical and Environmental Engineering, Technical University of Crete, Chania, 73100, Greece

Correspondence to: Konstantinos V. Varotsos (varotsos@noa.gr)

Abstract. We introduce the development of CLIMADAT-GRid, the first publicly available daily air temperature and precipitation gridded climate dataset for Greece at a high resolution of 1 km x 1 km, covering the period 1981–2019. The dataset is derived from quality-controlled and homogenized daily measurements from an extensive network of meteorological stations: 122 for temperature and 312 for precipitation. Several approaches are evaluated for generating the daily gridded datasets, and their accuracy is assessed against withheld observational data. To address the lack of observations in high-elevation areas, high-resolution simulations from the WRF model are blended with the observational data to provide the gridded temperature data. CLIMADAT-GRid is benchmarked against the CHELSA-W5E5, a global climate product with a similar resolution, for the overlapping period 1981–2016. While both datasets show comparable results for temperature, CLIMADAT-GRid demonstrates superior spatial variability and closer agreement with observational data for both the mean and for the extreme values. Regarding precipitation, CLIMADAT-GRid consistency indicates higher values than CHELSA, especially during the rainy season, but exhibits better agreement with observations. In terms of the number of wet days, both datasets overestimate spatial means relative to observations, with CLIMADAT-GRid showing a more pronounced orographic pattern than CHELSA. Both datasets show similar results for the number of days with precipitation amounts equal to or higher than 10 mm, with CLIMADAT-GRid indicating better overall agreement with the observations. The CLIMADAT-GRid dataset is publicly available at <https://doi.org/10.5281/zenodo.14637536> and can be cited as Varotsos et al. (2025).



30 1 Introduction

High-resolution gridded climate datasets, both spatially and temporally, are becoming a valuable resource for research and information in climate studies as well as in other areas such as hydrology, agriculture, energy and health (Herrera et al. 2012). In addition, high-resolution gridded datasets are used to evaluate, bias adjust and statistically downscale both regional and global climate models and seasonal forecasts (Lorenz et al., 2021; Nilsen et al., 2022; Varotsos et al., 2023a; Karali et al., 2023). Depending on the data sources and derivation techniques, gridded climate datasets can be divided into two main categories: (i) reanalysis datasets and (ii) gridded observational datasets. Reanalysis datasets provide a numerical description of the recent climate by combining dynamical models that assimilate observations, while gridded observational datasets are based on the statistical transformation of point meteorological station data into grid using geostatistical modelling.

As for the second category, which is the focus of this study, the remarkable advances in computing power and software have led to the development and creation of gridded observational datasets at both global and regional/national levels. In a recent study, Varotsos et al. (2023a) compiled a list of available observational gridded datasets for Europe, with E-OBS (Cornes et al., 2018) being the state-of-art gridded observational dataset for the entire European domain. However, it is crucial for users of gridded observational datasets to recognize that these products are model-generated rather than direct observations, and as such have a number of limitations (Hofstra et al., 2010). In particular, the quality of the gridded datasets depends on the quality of the station data and its spatial coverage (density of the meteorological station network), as interpolation methods degrade in performance in areas with sparse station data and/or in areas with complex topography (Hofstra et al., 2010; Begueria et al., 2016; Herrera et al., 2019).

Various gridding techniques for creating daily gridded datasets have been discussed in the existing literature. For instance, in the earlier versions of E-OBS (prior to v16, Haylock et al., 2008) and Iberia01 (Herrera et al., 2019), daily gridded datasets for temperatures (daily maximum, minimum and mean) and precipitation, were constructed using a trivariate thin-plate spline (using elevation as a covariate, Hutchinson et al., 2009) to construct monthly background field values (mean for temperatures and sums for precipitation), while the daily anomalies or proportions for temperatures and precipitation, respectively were interpolated using ordinary Kriging. To obtain the final daily gridded datasets the aforementioned fields were superimposed by addition and multiplication for temperatures and precipitation, respectively. In the latter versions of E-OBS (Cornes et al., 2018) the daily gridded datasets for temperatures and precipitation were constructed using Generalized Additive Models (GAMs, Wood, 2017) to estimate the long-range spatial trend in the data, while Gaussian Random Field simulation was used to interpolate the GAMs residuals. Other approaches include multiple linear regression, Delaunay triangulation and optimal interpolation (Nordic gridded temperature and precipitation data, NDCG, Tveito et al., 2000; Tveito et al., 2005; Lussana et al., 2018a, b). Furthermore, while machine learning (ML) has been successfully used to statistically downscale ERA5 (Qin et al., 2022; Hu et al., 2023) and climate change projections (Hernanz et al., 2024 and references therein), few studies, to our knowledge, have explored or evaluated the use of machine learning algorithms for generating observational gridded datasets. In particular, MeteoSerbia1km is a 1km horizontal daily gridded dataset for



temperatures, mean sea-level pressure, and total precipitation for the years 2000–2019, which was produced using the RFSI method, a spatial interpolation method based on the random forest ML algorithm (Sekulic et al., 2021). Moreover, Bonsoms and Ninyerola (2024) evaluated five ML techniques for the spatial interpolation of annual precipitation, minimum and maximum temperatures in the Pyrenees. The accuracy and performance of K-Nearest Neighbors, Supported Vector Machines, Neural Networks, Stochastic Gradient Boosting, and Random Forest were compared with those of multiple linear regressions and generalized additive models. According to the authors regardless of the elevation range, the geographical sector under analysis, or the predictor variables used, the ML algorithms outperformed multiple linear regressions and generalized additive models. Nevertheless, the authors did not proceed to the construction of a gridded dataset based on ML techniques. This is most likely due to the nature of ML techniques, which were designed for feature space qualities that cover almost all types of data and are therefore not commonly employed for spatial modeling (Nwaila et al., 2024).

In this study, we introduce CLIMADAT-GRid: a high-resolution (1 km x 1 km) daily gridded dataset for air temperatures (daily maximum, minimum and mean) and precipitation for Greece, covering the period 1981–2019 (Varotsos et al. 2025). To the best of our knowledge, this is the first publicly available dataset for Greece that offers daily gridded temperatures and precipitation in Greece at such fine spatial resolution. Previous studies known to the authors have primarily focused on monthly values of these variables for the 1971–2000 period (Mamara et al., 2017; Gofa et al., 2019).

2 Data

2.1 Daily observational data for maximum (*TX*), minimum (*TN*), mean (*TG*) temperatures and daily precipitation sums (*PR*)

This study utilizes daily air temperature observations from two main sources. The first is the National Observatory of Athens Automatic Network (NOAAN, Lagouvardos et al., 2017), which provides records from 48 stations for the period 2010–2019, and the second source is Hellenic National Meteorological Service (HNMS), which provides temperature records from 73 stations spanning 1981–2019. In addition, we incorporate daily observations from the historical weather station of the National Observatory of Athens in Thissio (NOA) for the same period. In total, daily data from 122 meteorological stations across Greece were collected (Fig. 1a), with station altitude ranging from 1 to 960 m above sea level (a.s.l.).

In addition to the data from the stations mentioned above, we also collected daily precipitation data for 190 stations provided by the General Secretariat for Natural Environment and Water of the Ministry of Environment and Energy for the period 1981–2019. In total, daily precipitation sums of 312 stations are obtained (Fig. 1b), with altitudes from sea level to 1130 m a.s.l. The selected stations were included based on the criterion of having less than 10 % missing data on an annual basis.



95

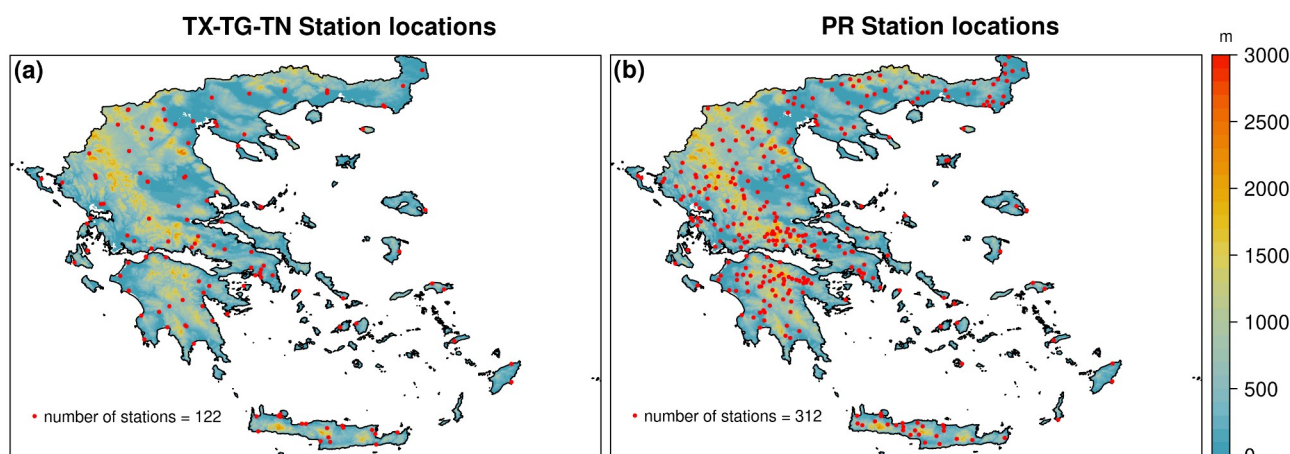


Figure 1. Locations of meteorological stations for (a) temperatures and (b) precipitation measurements. Background shows elevation data as from the Global Multi-resolution Terrain Elevation Data 2010 (GMTED2010).

2.2 Quality control, gap filling and homogenization

100 An initial quality control for all variables was conducted using the R package *climatol* (version 4.1.1, Guijarro, 2023), which automatically identifies and discards all extreme anomalies and removes prolonged sequences of identical values from data. As for daily precipitation, which has a significantly skewed frequency distribution, the deletion of high isolated data is not permitted because heavy rain can occur between two days with little or no precipitation. In addition, zero values of daily precipitation are automatically excluded so that days with no precipitation are not included in the analysis of sequences with
 105 identical data.

For temperatures, the gap filling and homogenization were carried out following the methodology of Varotsos et al. (2023b). This method reconstructs missing daily temperatures values (*TX*, *TG* and *TN*) over an extended period of time, using *climatol* R package, station data and the ERA5-Land reanalysis dataset (Muñoz-Sabater et al., 2021). Since this method is capable of reconstructing temperatures both forward and backward in time, it was selected to provide consistent and homogenized data
 110 for the period 1981–2019 across all 122 available stations. For further details on the methodology, the reader is referred to the work of Varotsos et al. (2023b).

For precipitation, gap filling and homogenisation were carried out in two phases. In the first phase, stations covering the period 1981–2019 (including HNMS stations, the Ministry of Environment and Energy network, and the historical Thissio NOA station) were post-processed using *climatol* package, with data from the nearest station serving as the reference. In the
 115 second phase, the homogenised data series for the period 2010–2019 were used to fill gaps and homogenise the daily precipitation data of the NOAA network. Following these procedures, the total number of precipitation data series is 264 for 1981–2010 and 312 for 2010–2019.



2.3 WRF simulations

For the atmospheric simulations, the Advanced Weather Research and Forecasting Model (WRF-ARW) version 4.1.3 (Powers et al., 2017; Skamarock et al., 2008; Skamarock et al., 2019) was employed. WRF-ARW serves as a limited-area atmospheric model, utilized for both operational forecasting (Sofia et al., 2024; Patlakas et al., 2023) and scientific research (Stathopoulos et al., 2023; Otero-Casal et al., 2019). It is based on a fully compressible, non-hydrostatic dynamic core. On the vertical plane it has terrain-following, mass-based, hybrid sigma-pressure vertical coordinates based on dry hydrostatic pressure, with vertical grid stretching permitted while for the horizontal grid, the Arakawa C-grid staggering is employed.

In this analysis, the WRF model was configured to run with three two-way nested grids. The coarser one has a resolution of 9 km, covering a large area that includes parts of North Africa and Central Europe. The inner grids are focused on the Eastern Mediterranean and Greece, with spatial resolutions of 3 km and 1 km, respectively. Vertically, the model consists of 48 layers.

The main physics options and parameterizations used are summarized in the next table (Table 1).

Table 1: WRF model physical schemes and properties.

Microphysics	Thompson scheme (Thompson et al., 2004)
Cumulus Parameterization	Kain–Fritsch scheme (Kain, 2004)
Long wave radiation physics	RRTMG scheme (Iacono et al., 2008)
Short wave radiation physics	RRTMG scheme
Planet boundary layer	Yonsei University (YSU) PBL scheme (Hong et al., 2006)
Surface layer option	Monin–Obukhov similarity scheme
Land-surface physics	Thermal Diffusion scheme

For the initial and the boundary conditions, the ERA-5 (Hersbach et al., 2020) hourly data has been incorporated. This is the latest global atmospheric reanalysis product produced by the European Centre for Medium-Range Weather Forecasts (ECMWF), covering the period from 1940 to the present with continuous real time updates and a spatial resolution of approximately 0.25 degrees. Terrain elevation data is obtained from the ASTER Global Digital Elevation Map (GDEM) from USGS (United States Geological Survey) (Slater et al., 2011) with a resolution of 30 m, and land use information from the Corine (Coordination of Information on the Environment) database (2010) at a 250 m resolution.

Following the approach of Varotsos et al. (2023a), the year selected for the WRF simulation was chosen based on its mean monthly annual cycle, the lowest deviations from its long-term mean for the period 1981–2019. The analysis revealed that the year 1999 had the lowest temperature and precipitation deviations, from the long-term mean.



3 Methodology

The methodology applied in this study to produce the daily gridded observational precipitation dataset for Greece for the years 1981–2019, aligns to that used in the early versions of E-OBS (Haylock et al., 2008) and IBERIA01 (Herrera et al., 2019). For temperature variables we adopted and extended the methodology described by Varotsos et al. (2023a), where the available observed data were blended with WRF output through gridding techniques. While Varotsos et al. (2023a) focused on Attica region, we expanded their methodology to cover the entire Greek territory. This blending approach was selected over using only the observational data to better account for temperature gradients driven by topography, particularly since our observational dataset lacks stations located above 1000 m a.s.l.

3.1 Spatiotemporal modeling for precipitation

The steps to obtain the daily grids for precipitation are as follows:

- interpolation of monthly totals (12 values \times 39 years) using altitude as a covariate to account for altitude dependencies (station altitude for modeling and GMTED2010, 30 arcsec version, altitude for interpolation).

The following approaches were examined to calculate the monthly precipitation fields: (i) a “fixed rank Kriging approach” (hereafter FRK, Nychka et al., 2015), (ii) generalized additive models (hereafter GAM, Wood, 2017) and (iii) two ML algorithms namely k-nearest neighbors (hereafter KNN) and support vector machines (hereafter, SVM). The analysis is performed using the R Language and Environment for Statistical Computing (R core team 2024) and the packages LatticeKrig (Nychka et al., 2019) for FRK, mgcv (Wood and Wood, 2015) for GAM, while the two ML algorithms are tuned using the caret R package (Kuhn, 2008). The choice of these two ML algorithms was based on literature (e.g., Bonsoms and Ninyerola, 2024), as well as on preliminary tests that included other algorithms, such as random forests, gradient boosting machines and neural networks. However, the latter algorithms were excluded as they produced unrealistic cross-hatched patterns in the precipitation background fields.

- interpolation of the daily anomalies (quotient from the monthly total values, 365 values/year \times 39 years) of the observational data.

The final step of precipitation interpolation was implemented using an exponential covariance with the covariance parameters estimated through maximum likelihood. For more information, the reader is referred to the fields R package spatialProcess function (Nychka et al., 2015). To obtain the final daily gridded dataset for precipitation, the two interpolated precipitation products obtained are superimposed by multiplication.

3.2 Spatiotemporal modeling for temperatures

As outlined earlier in Sect. 3, the methodology of Varotsos et al. (2023a) was applied to generate the daily gridded temperature datasets with the key steps as implemented in this work briefly summarized below.



The approach is implemented in four steps. The first two steps involve the WRF perturbation to align with observed long-term climate temporal characteristics while preserving its spatial variability. This is achieved by adding the interpolated monthly biases, calculated as the difference between the mean monthly annual cycles over the period 1981–2019 and the monthly means calculated over the year 1999 at the closest WRF grid point to each station location, to the mean monthly values at each grid point. The third step involves the construction of the gridded dataset following the first two steps mentioned for the precipitation dataset by adding the interpolated mean monthly values, derived by the different methods (FRK, GAM, KNN, SVM) with the interpolated daily anomalies calculated as the difference between the daily observation and the monthly mean. The last step involves the transfer of perturbed WRF output to the daily gridded dataset of the previous step using the unbiasing bias adjustment method (Déqué, 2007).

3.3 Evaluation analysis against withheld station data

An evaluation of the different approaches for constructing the daily grids was conducted for the test period (2010–2019). The aim of this evaluation was to identify the most effective method for generating daily datasets for all variables over the period 1981–2019. To achieve this, approximately 10 % of the stations were excluded from the dataset, and the interpolated values were compared with the observed values at those locations. For both temperatures and precipitation station data, the withheld stations were selected using the minimax distance design (Johnson et al., 1990; Cornes et al., 2018), which minimizes the maximum distance from each withheld station to any of the other stations (Fig. 2a and 2b).

The accuracy of the various approaches is assessed using Root Mean Square Error (RMSE), Mean Absolute Error (MAE), and Kling-Gupta Efficiency (KGE) measures. The KGE metric is a measure of goodness of fit that has been routinely used to evaluate climate datasets (Beck et al., 2019; Bhuiyan et al., 2019; Avila-Diaz et al., 2021). KGE can obtain values ranging from $-\infty$ to +1, with values of +1.0 and -1.0 to indicate perfect positive and negative linear correlation between the reference and the assessed timeseries, respectively, while a value of 0 implies no correlation. In this study, gridding techniques are more accurate when KGE values are close to one. When calculating the KGE, three key factors are considered: (i) the Pearson product-moment correlation coefficient (R), (ii) the ratio of the mean of the reconstructed values to the mean of the observed values (β), and (iii) the variability ratio based on the standard deviations of the reconstructed values to the observed values (α).

3.4 Comparison against CHELSA-W5E5

The final produced daily gridded datasets for temperatures and precipitation were compared against the corresponding variables from CHELSA-W5E5 v1 (hereafter CHELSA, Karger et al., 2023). CHELSA is a 1 km daily global land dataset for air temperatures, precipitation rates, and downwelling shortwave solar radiation for the period 1979–2016 and has been produced by spatially downscaling the 0.5° W5E5 dataset on an identical resolution grid as the one used in this study (GMTED2010). Moreover Papa and Koutroulis (2025,) found that CHELSA is one of the two more reliable gridded datasets for describing the precipitation dynamics in Greece. The comparison was performed by examining average annual and



seasonal means for all temperature variables (sums for precipitation), as well as selected indices from the Expert Team on
Climate Change Detection and Indices (ETCCDI) (Zhang et al. 2011). These are the number of days with daily $TX > 25^{\circ}\text{C}$
(SU) and $TX > 35^{\circ}\text{C}$ (SU35) for TX , the number of days with daily $TN > 20^{\circ}\text{C}$ (TR) for TN and the number of days with PR
 $> 1\text{ mm}$ (RR1) as well as the number of days with $PR \geq 10\text{ mm}$ (RR10mm) for PR . These indices were selected considering
the primary climatic characteristics of the studied area, which exhibits Mediterranean-type climate conditions with moderate
winters and warm to hot summers.

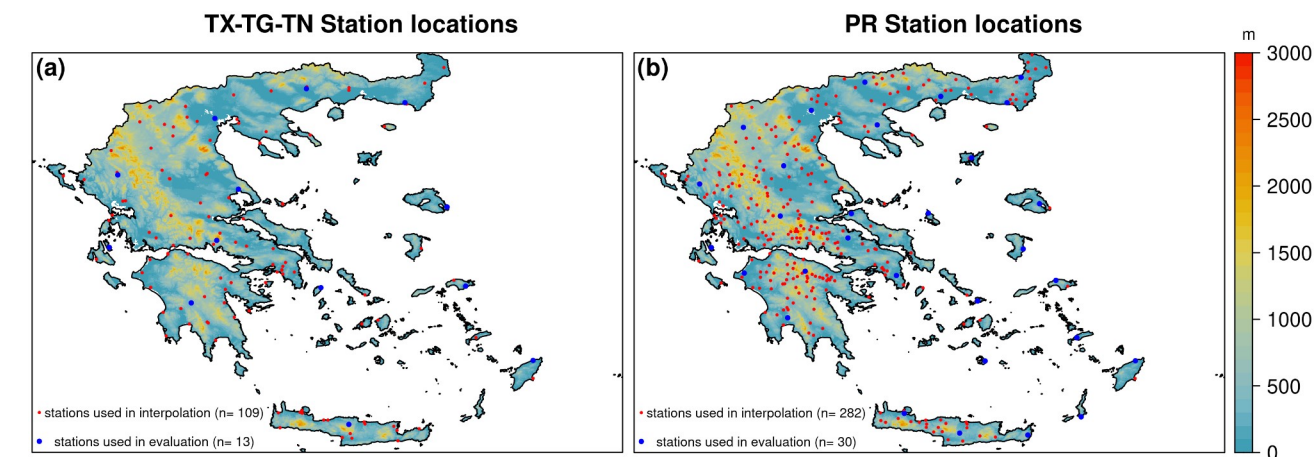


Figure 2. Stations used in the interpolation as well as withheld station data during the evaluation analysis for (a) temperatures and (b) precipitation. In the background the elevation as provided by GMTED2010.

4 Results

4.1 Evaluation against withheld station data for the test period (2010–2019)

4.1.1 Precipitation results

The values of the root mean square error (RMSE), the mean absolute error (MAE) and the KGEs are presented in Table 2 for
the precipitation grids produced using the different approaches described in Sect. 3.1. These results are compared against the
withheld observations on an annual and seasonal basis for the test period. From Table 2 it is clear that the methods yield
similar values across all statistical measures with annual RMSE (MAE) being lower than 1.45 (0.65) for all methods. On a
seasonal basis, the highest RMSE and MAE are observed during the DJF (December-January-February) and SON
(September-October-November) periods. Overall, SVM and FRK methods exhibit the lowest values for both metrics on an
annual and seasonal basis. Regarding the KGEs, with the exception of GAMs that exhibit a KGE value of 0.7 in JJA (June-
July-August), for the rest of the seasons and on an annual basis the reported KGEs are higher than 0.8. Similar to RMSEs
and MAEs, the highest KGE values are found for the SVM and FRK methods indicating that these two methods capture
quite well the temporal distributions of the daily precipitation.



In Fig. 3 the average annual daily distributions for precipitation are shown for the 10 years test period. The results indicate that the methods can capture the annual total precipitation, with the maximum relative absolute biases of 8 % or less across all methods.

230

Table 2: Precipitation annual and seasonal RMSE, MAE and KGE statistics between the 30 reference station values and the interpolated ones as derived from the different interpolation approaches.

	FRK			GAM			KNN			SVM		
PR	RMSE	MAE	KGE	RMSE	MAE	KGE	RMSE	MAE	KGE	RMSE	MAE	KGE
Annual	1.13	0.60	0.92	1.45	0.63	0.87	1.18	0.62	0.87	1.09	0.59	0.93
DJF	1.51	0.95	0.88	1.46	1.01	0.81	1.56	0.97	0.84	1.43	0.91	0.91
MAM	0.94	0.50	0.90	1.47	0.93	0.88	0.99	0.54	0.86	0.92	0.51	0.92
JJA	0.65	0.29	0.82	1.47	0.3	0.70	0.63	0.29	0.86	0.67	0.31	0.82
SON	1.27	0.66	0.93	1.43	0.71	0.87	1.34	0.69	0.85	1.22	0.66	0.94

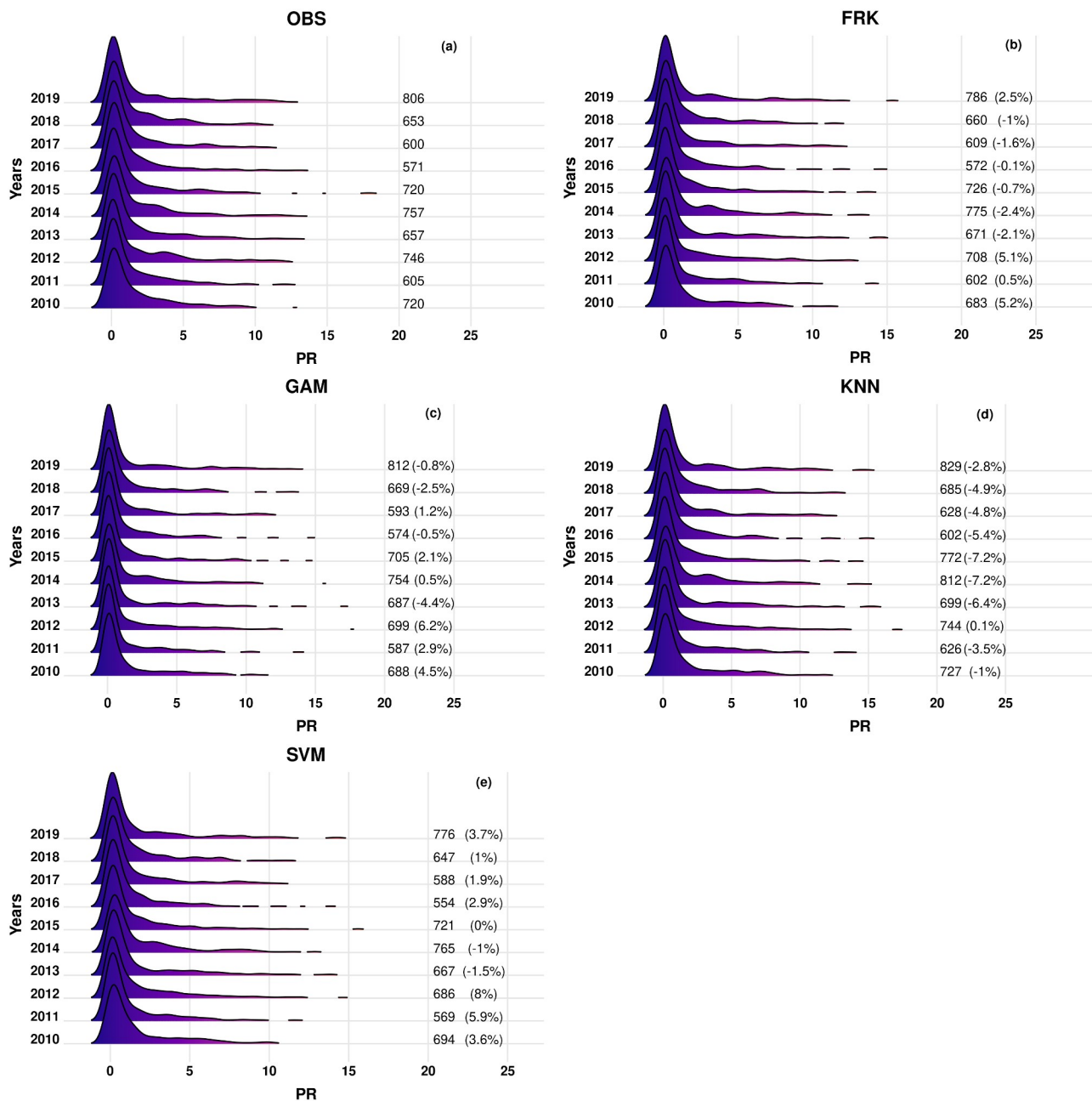


Figure 3. Density distributions of daily precipitation values over the withheld station data for the observations (OBS) and the different methods used for interpolation for the years 2010–2019. The values shown in the plots are the total annual precipitation values whereas the relative biases between the different methods and the observations are shown in parenthesis.

In terms of spatial distribution, the west to east gradient of precipitation in Greece, which exhibits the largest and lowest amounts of yearly precipitation (Gofa et al., 2019), is captured by all approaches. However, as Fig. 4 for the year 2016 illustrates, GAM, KNN and SVM demonstrate reduced spatial variability in regions with significant altitude differences in



both the northeastern and southern regions of Greece (e.g. Crete). This spatial variability is also evident in other years examined within the 2010–2019 period (not shown).

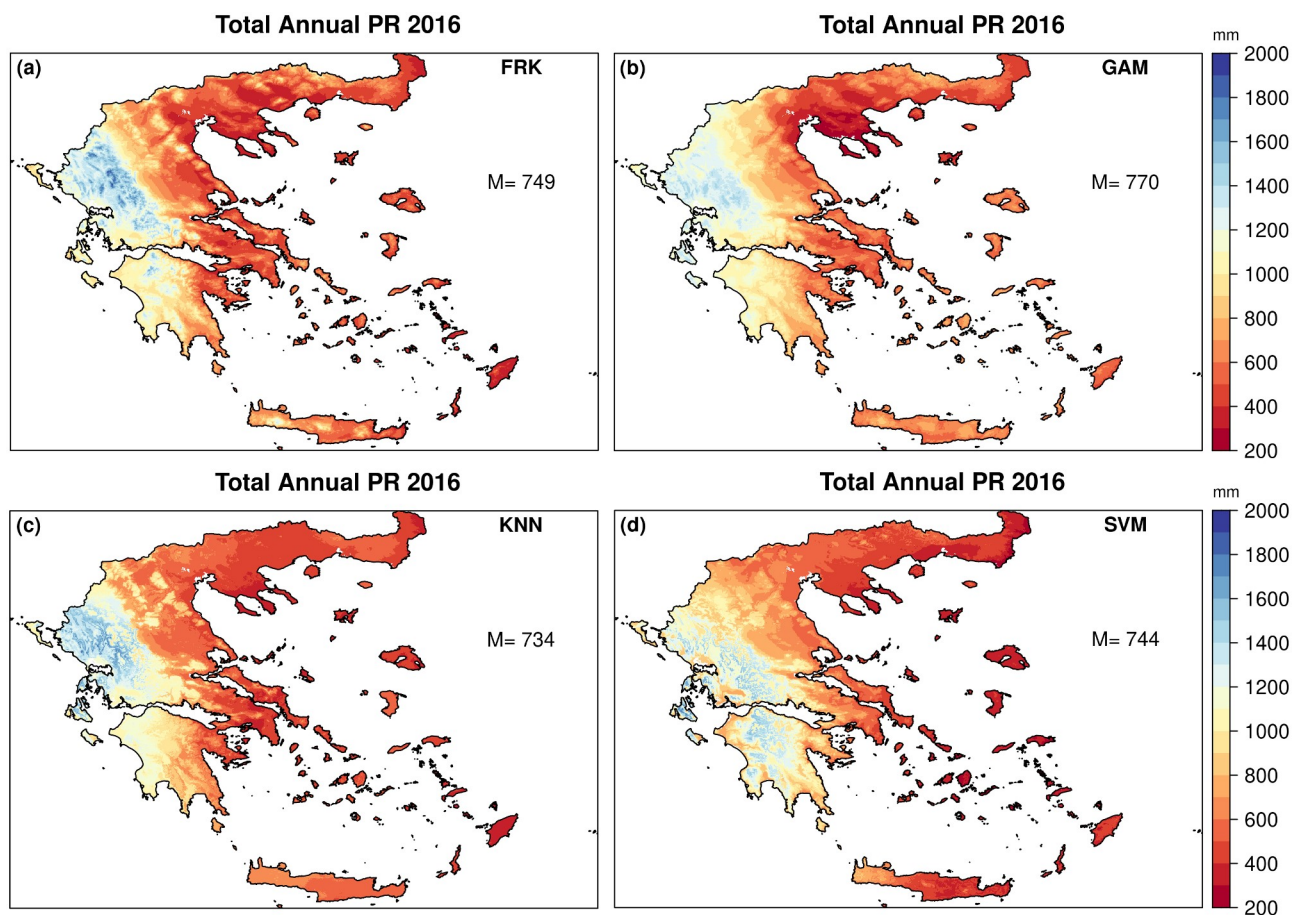


Figure 4. Spatial distribution of total annual precipitation for the year 2016 as obtained from the different methods used for interpolation. In each panel, M denotes the spatial average over all grid points.

4.1.2 Temperature results

This section is dedicated to the evaluation of the effectiveness of the proposed approaches in reproducing observed temperatures, specifically addressing the third phase of the temperature methodology described in Sect. 3.2.

From Table 3 and Fig. 5-7, it is evident that all methods perform well in capturing the temporal temperature characteristics for *TX*, *TG* and *TN*. For *TX* the methods yielding the best performance in terms of RMSE, MAE and KGE are KNN and SVM. KNN shows better performance during the colder seasons (DJF and SON), while SVM in the warmer ones (March-April-May (MAM) and JJA). FRK is the third best performing method, while GAM exhibits the highest RMSEs at all periods examined. Considering the annual biases (Fig. 5) a different perspective emerges. GAM shows the lowest absolute



biases (below 0.2 °C), while FRK displays the highest biases (up to 0.6 °C), highlighting variations in the strengths of the methods depending on the evaluation metric.

For *TG* and *TN*, FRK emerges as the best-performing method across all metrics on both an annual and seasonal basis, consistently exhibiting the lowest RMSE, MAE and KGE values with the rest of the methods having comparable performance, with the exception of the higher RMSE values obtained by GAM. In addition, FRK values exhibit the lowest mean absolute annual deviations from the observed values, lower than 0.3 °C, for both *TG* and *TN*, while for the rest of the methods these deviations may reach 0.8 °C depending on the method and variable (Fig. 6 and 7, respectively).

Table 3: Daily maximum (*TX*), mean (*TG*) and minimum (*TN*) temperatures annual and seasonal RMSE, MAE and KGE statistics between the 13 reference station values and the interpolated ones as derived from the different interpolation approaches.

	FRK			GAM			KNN			SVM		
	RMSE	MAE	KGE	RMSE	MAE	KGE	RMSE	MAE	KGE	RMSE	MAE	KGE
<i>TX</i>												
Annual	0.69	0.55	0.98	1.63	0.48	0.98	0.60	0.50	0.98	0.60	0.49	0.98
DJF	0.68	0.55	0.91	1.6	0.41	0.93	0.60	0.49	0.93	0.64	0.53	0.94
MAM	0.60	0.47	0.97	1.53	0.53	0.97	0.67	0.56	0.98	0.62	0.51	0.98
JJA	0.72	0.58	0.97	1.35	0.49	0.98	0.60	0.50	0.98	0.56	0.46	0.98
SON	0.76	0.61	0.96	1.48	0.47	0.98	0.55	0.45	0.99	0.57	0.46	0.98
<i>TG</i>												
Annual	0.45	0.36	0.98	2.81	0.48	0.97	0.69	0.59	0.97	0.82	0.73	0.96
DJF	0.45	0.36	0.98	2.56	0.38	0.97	0.67	0.56	0.93	0.77	0.66	0.92
MAM	0.45	0.36	0.97	2.43	0.57	0.96	0.75	0.67	0.95	0.80	0.71	0.95
JJA	0.48	0.37	0.97	2.32	0.55	0.97	0.66	0.57	0.97	0.88	0.79	0.96
SON	0.42	0.35	0.96	2.53	0.43	0.97	0.67	0.58	0.97	0.83	0.74	0.96
<i>TN</i>												
Annual	0.52	0.41	0.99	3.85	0.59	0.96	0.88	0.77	0.94	0.77	0.64	0.95
DJF	0.63	0.52	0.92	3.85	0.58	0.88	0.97	0.80	0.80	0.93	0.75	0.82
MAM	0.52	0.43	0.98	3.85	0.70	0.93	0.88	0.78	0.92	0.72	0.60	0.95



JJA	0.42	0.34	0.98	3.79	0.57	0.97	0.83	0.73	0.96	0.65	0.54	0.95
SON	0.48	0.38	0.99	3.85	0.54	0.96	0.88	0.77	0.94	0.79	0.68	0.95

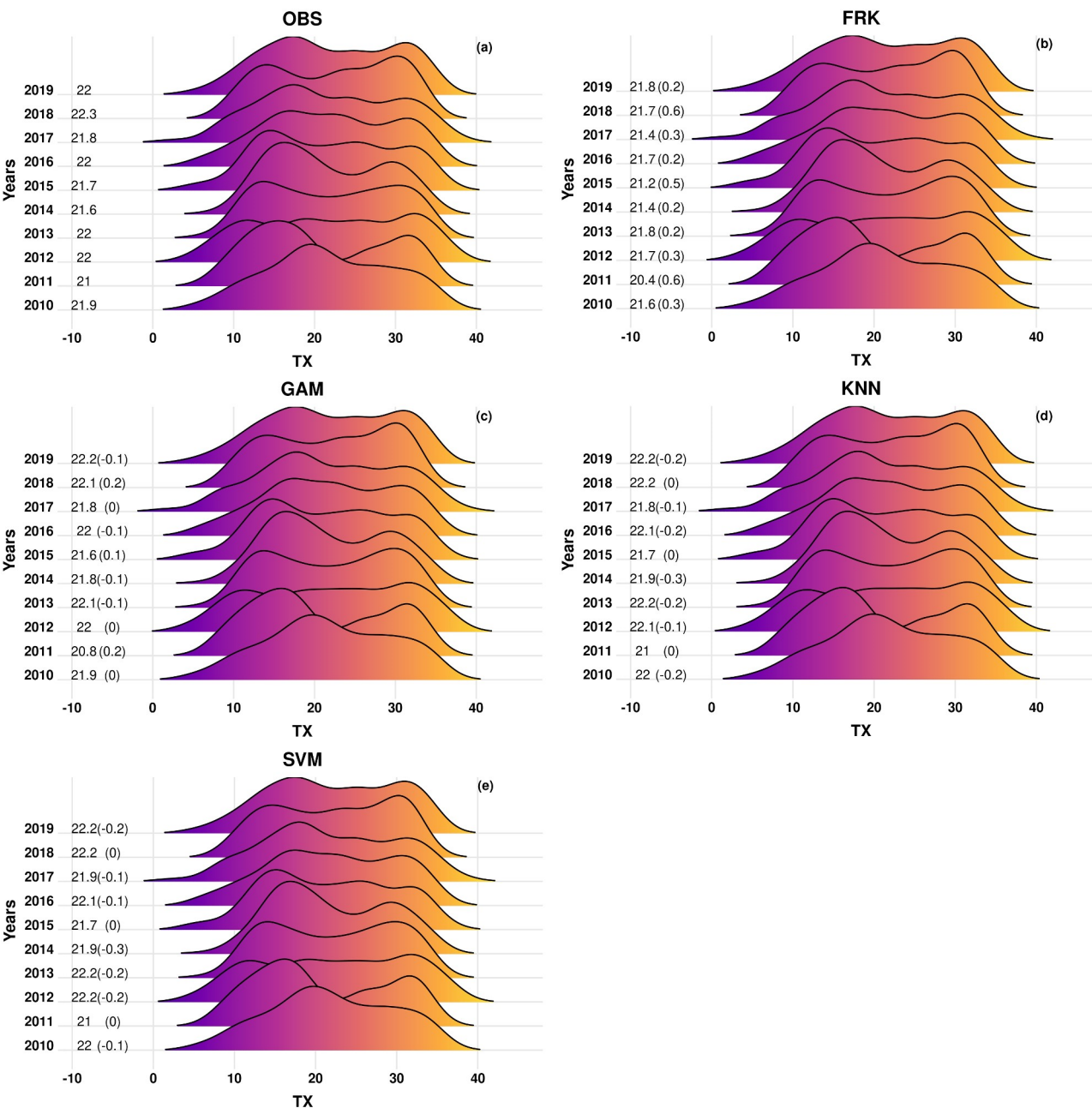


Figure 5. Density distributions of daily maximum temperature (TX) values over the withheld station data for the observations (OBS) and the different methods used for interpolation for the years 2010-2019. The values shown in the plots are the average annual values whereas the biases between the different methods and the observations are shown in parenthesis.

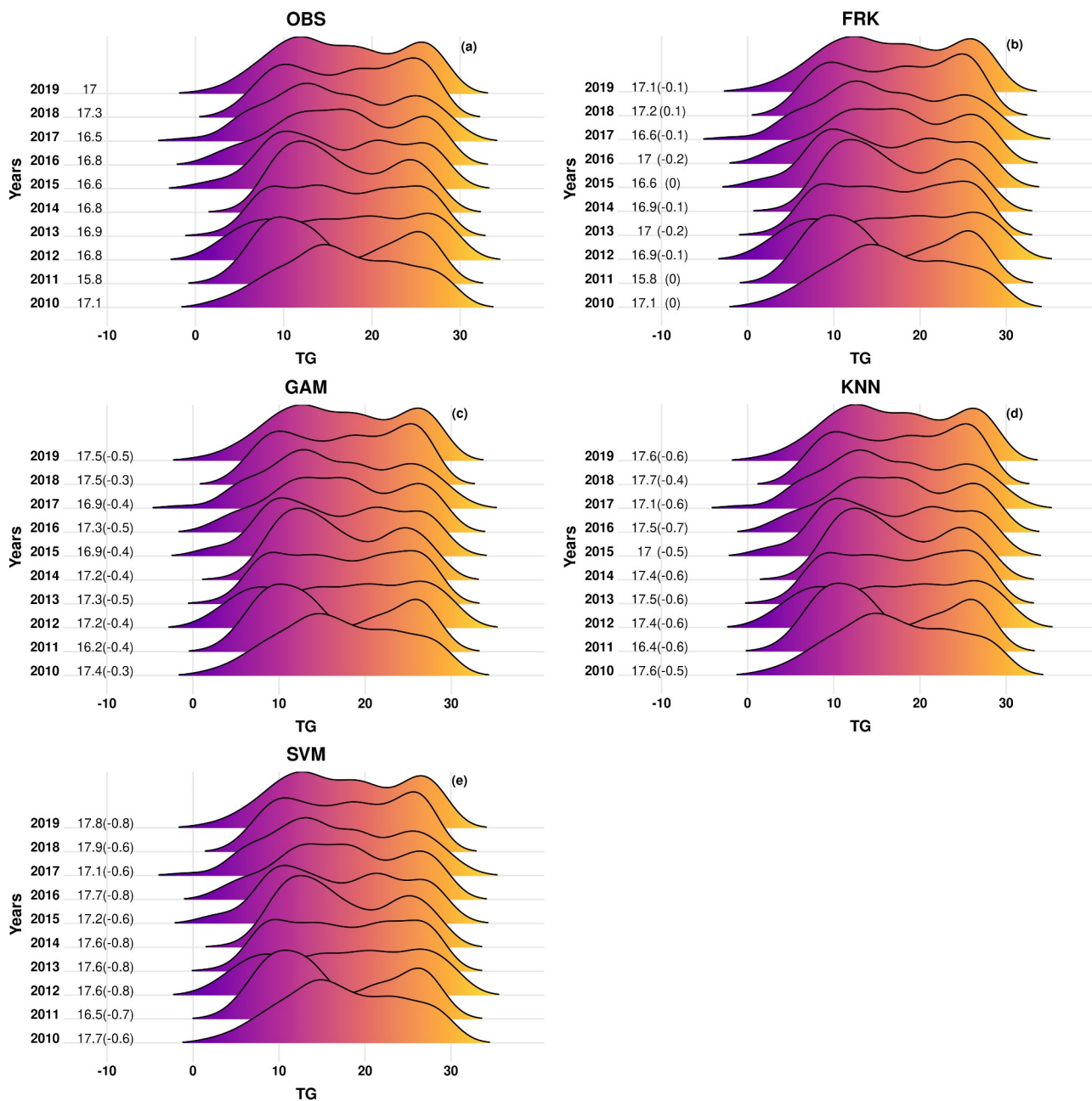


Figure 6. Density distributions of daily mean temperature (*TG*) over the withheld station data for the observations (OBS) and the different methods used for interpolation for the years 2010-2019. The values shown in the plots are the average annual values whereas the biases between the different methods and the observations are shown in parenthesis.

275

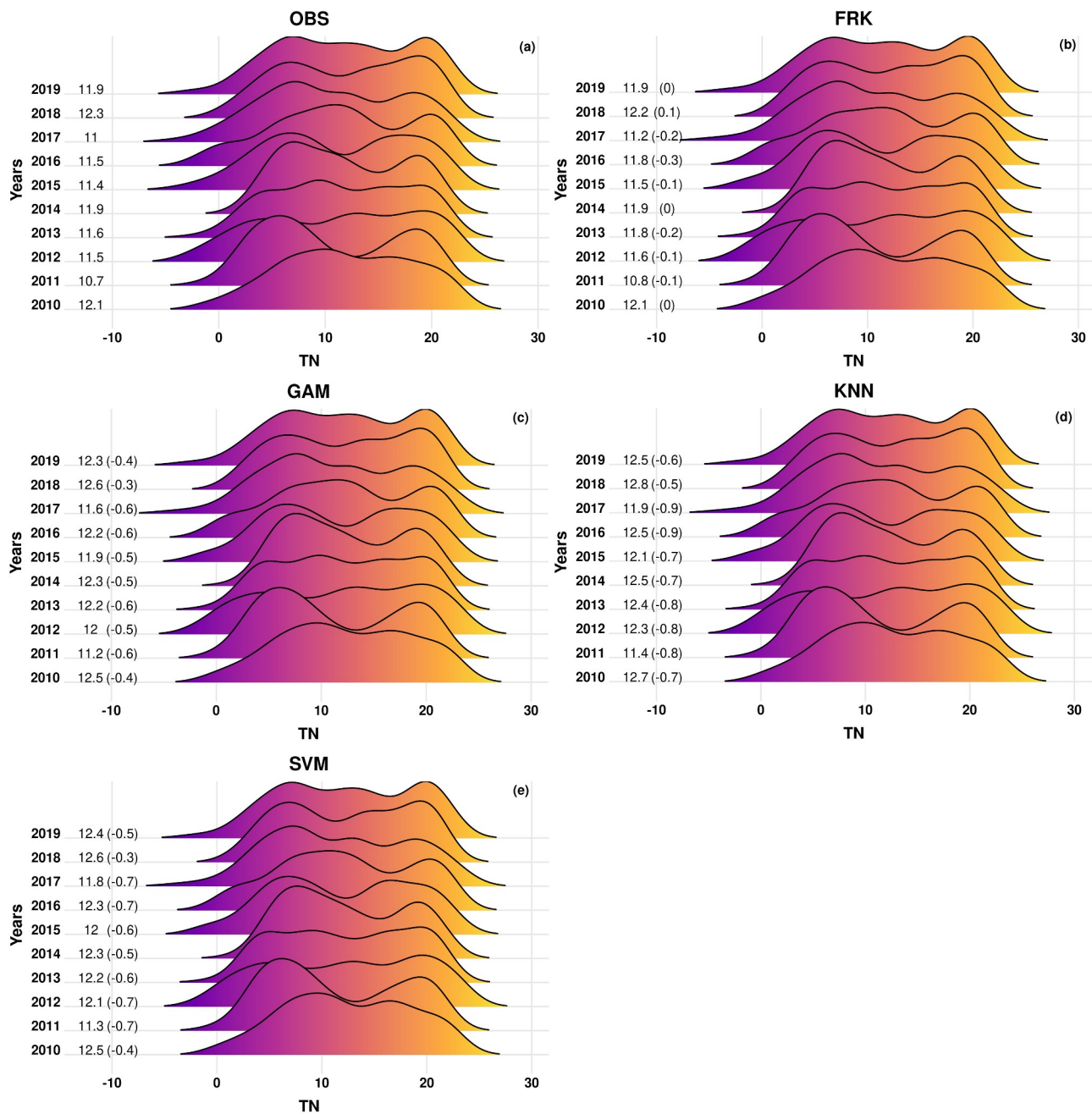


Figure 7. Density distributions of daily minimum temperature (*TN*) values over the withheld station data for the observations (OBS) and the different methods used for interpolation for the years 2010-2019. The values shown in the plots are the average annual values whereas the biases between the different methods and the observations are shown in parenthesis.



285 In terms of spatial distribution, similar patterns to those observed for precipitation are identified. In particular GAM, KNN and SVM demonstrate reduced spatial variability between the mountainous areas of Greece and the lower altitude surrounding areas indicating limited ability to accurately represent temperature gradients influenced by topography (not shown).

Based on the above analysis performed for precipitation and temperature variables, we opt to proceed with the development of the daily grids using the FRK method for gridding the mean and total monthly values for temperatures and precipitation, respectively with the final dataset CLIMADAT-GRid covering the period 1981–2019.

4.2 Results of the comparison between CLIMADAT-GRid against CHELSA-W5E5 for the period 1981–2016

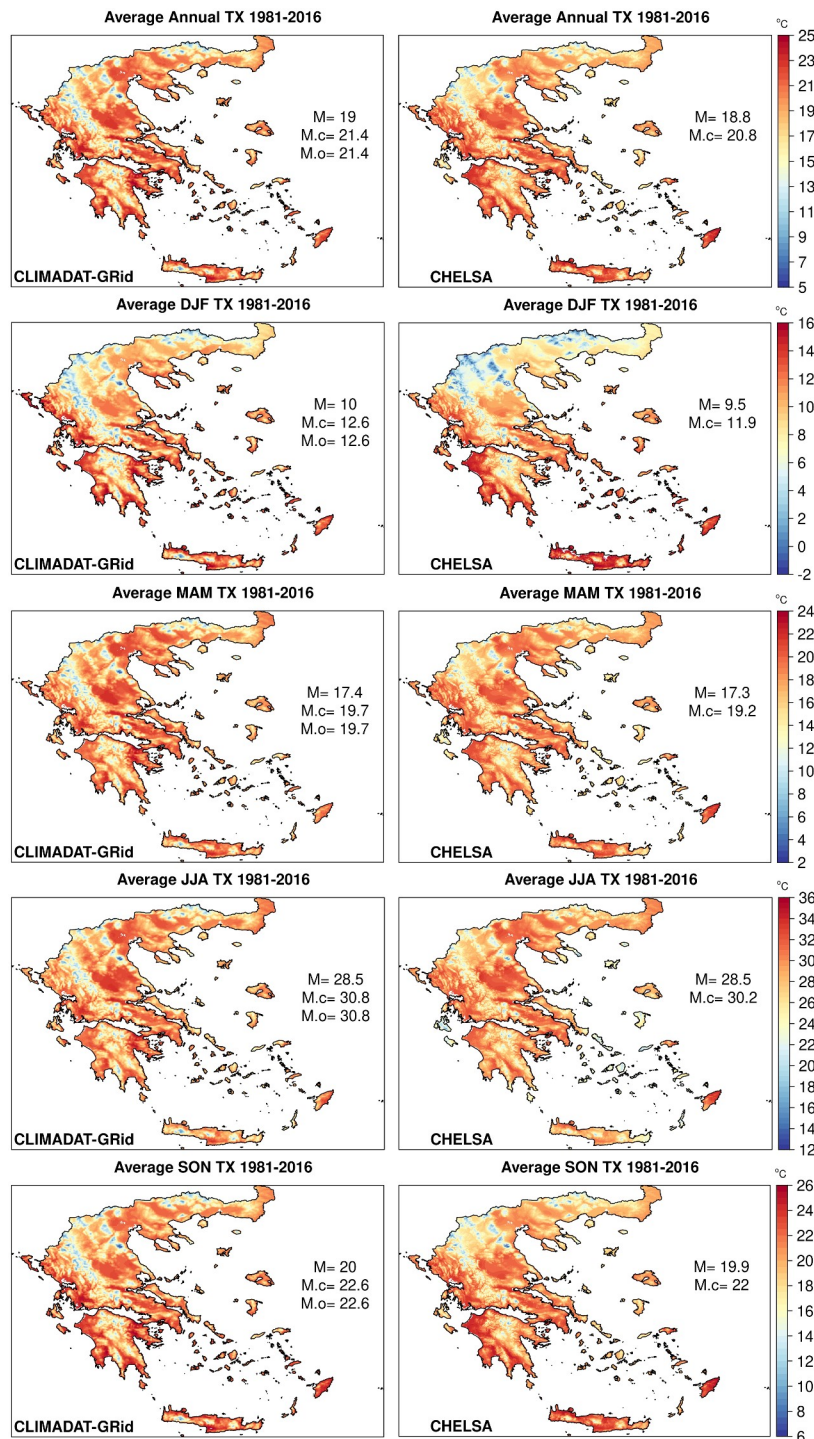
4.2.1 Daily maximum and minimum temperature results

295 In Fig. 8 and 9 the average annual and seasonal temperature results for TX and TN are shown, respectively. For TX , both datasets show comparable temperature values averaged over the whole domain of interest (denoted as M in the figures), with the maximum difference between the two datasets not exceeding 0.5 °C (DJF). When compared to the station data (M.o in the figures) CLIMADAT-GRid exhibits values of similar magnitude for the closest grid point to the station locations (M.c in the figures), while CHELSA systematically underestimates the observations on both the annual and the seasonal timescales, with average discrepancies between 0.5 °C to 0.7 °C. In terms of spatial variability, CLIMADAT-GRid with WRF blended in the gridded dataset better captures the orographical gradient of temperatures, indicating lower temperatures than CHELSA in mountainous areas ranging from the northwest of Greece to the central Peloponnese and west of Crete. Furthermore, CHELSA appears to be cooler than CLIMADAT-GRid in the Ionian Sea islands of Zakynthos and Kefallonia, as well as the Aegean sea islands of Cyclades, but warmer in Rhodes and Samos.

305 For TN (Fig. 9), both datasets show nearly identical temperature values averaged across the entire domain of interest, with the highest difference between them not exceeding 0.2 °C (MAM and SON). CLIMADAT-GRid produces values of the same magnitude as the station data for the grid points nearest to the station locations, whereas CHELSA slightly overestimates the observations annually, DJF and MAM. Nonetheless, the maximum overestimation in daily minimum temperatures is less than 0.3 °C. In contrast, JJA and SON produce temperatures that are similar to those observed. The highest discrepancy between the two datasets is obvious while examining the maps in Fig. 8. In particular, CHELSA indicates notably higher temperatures compared to CLIMADAT-GRid, from west to east, in the Ionian Sea's Zakynthos and Kefallonia, as well as Crete, and the majority of the Aegean Sea islands. The higher temperatures in CHELSA can be attributed to the implementation of a basic statistical downscaling approach that employs atmospheric temperature lapse rates, B-spline interpolations, and high-resolution orography rather than a full physical scheme (Karger et al., 2023). Furthermore, according to the authors, constant lapse rates were utilized for all air temperature variables impacting minimum temperatures to a greater extent, as minimum temperatures in high altitudes are frequently the result of nighttime inversions.



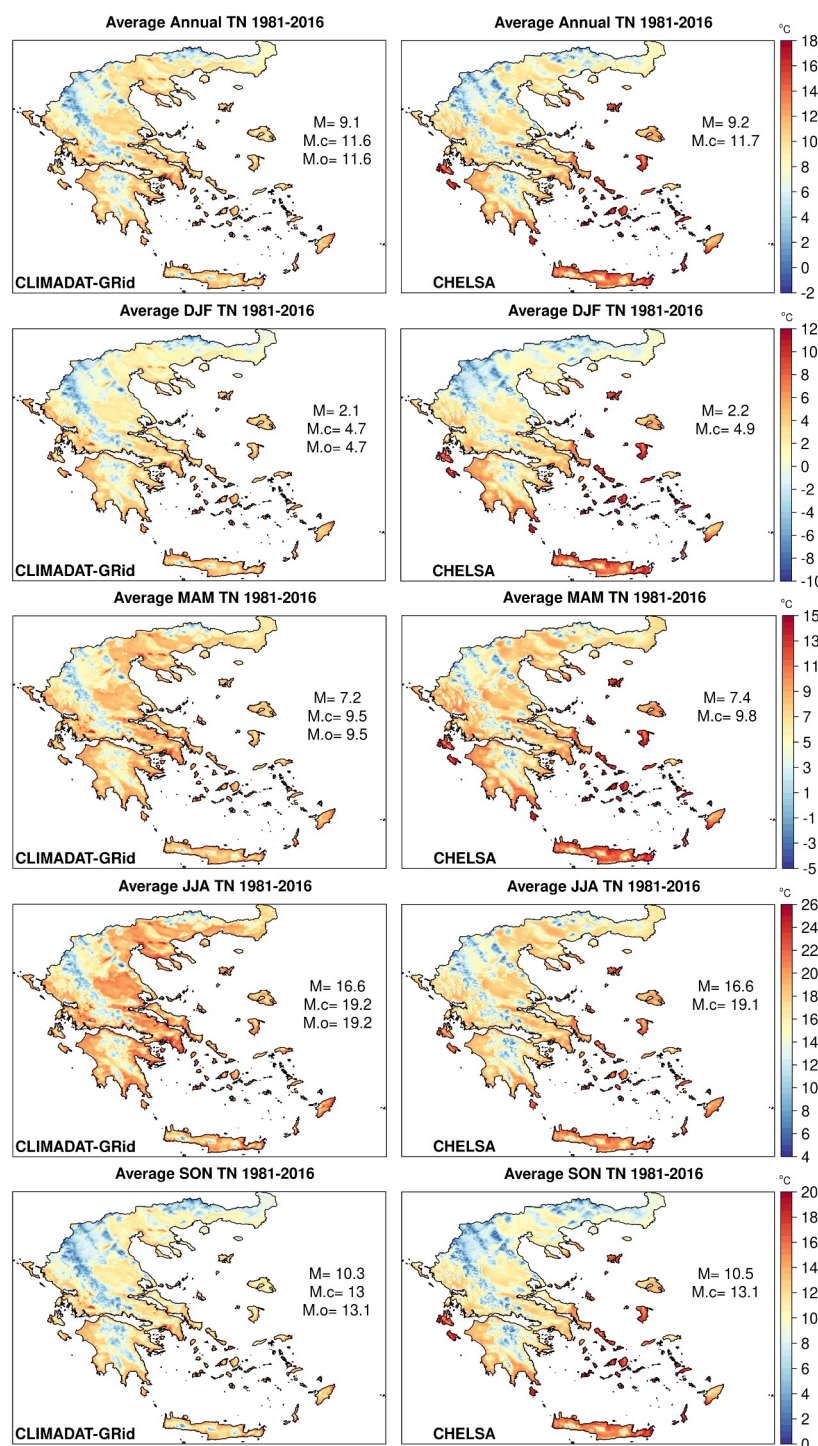
Figure 10 illustrates the results for the number of days with daily $TX > 25^{\circ}\text{C}$ (SU) and $TX > 35^{\circ}\text{C}$ (SU35) and the number of days with daily $TN > 20^{\circ}\text{C}$ (TR). From the figure it is evident that both datasets yield similar domain averaged values for SU and SU35. However, for TR, CHELSA estimates a higher number of days/yr compared to CLIMADAT-GRid (23 and 18 days/yr, respectively). Despite this, CHELSA underestimates the observed number of SU by about 10 days/yr, while CLIMADAT-GRid closely aligns with the observed values. Differences are most noticeable in the spatial variability of the results, which are most evident in the Ionian Sea Zakynthos and Kefallonia islands, as well as the Aegean Sea Cyclades for SU and in the Ionian Sea Zakynthos and Kefallonia islands, as well as Crete and the majority of the Aegean Sea's islands for TR. Furthermore, CLIMADAT-GRid catches pretty well the spatial variability of SU35, pinpointing well-known warm hot spots in the Greek territory, as well as the urban heat island effect in the Athens urban area, which is also evident in CHELSA, but to a lesser extent.



330 Figure 8. Average annual and seasonal TX (winter (DJF), spring (MAM), summer (JJA) and autumn (SON)) for the period 1981–2016 for CLIMADAT-GRid (left column) and CHELSA (right column). In each panel, M denotes the spatial average over the grid

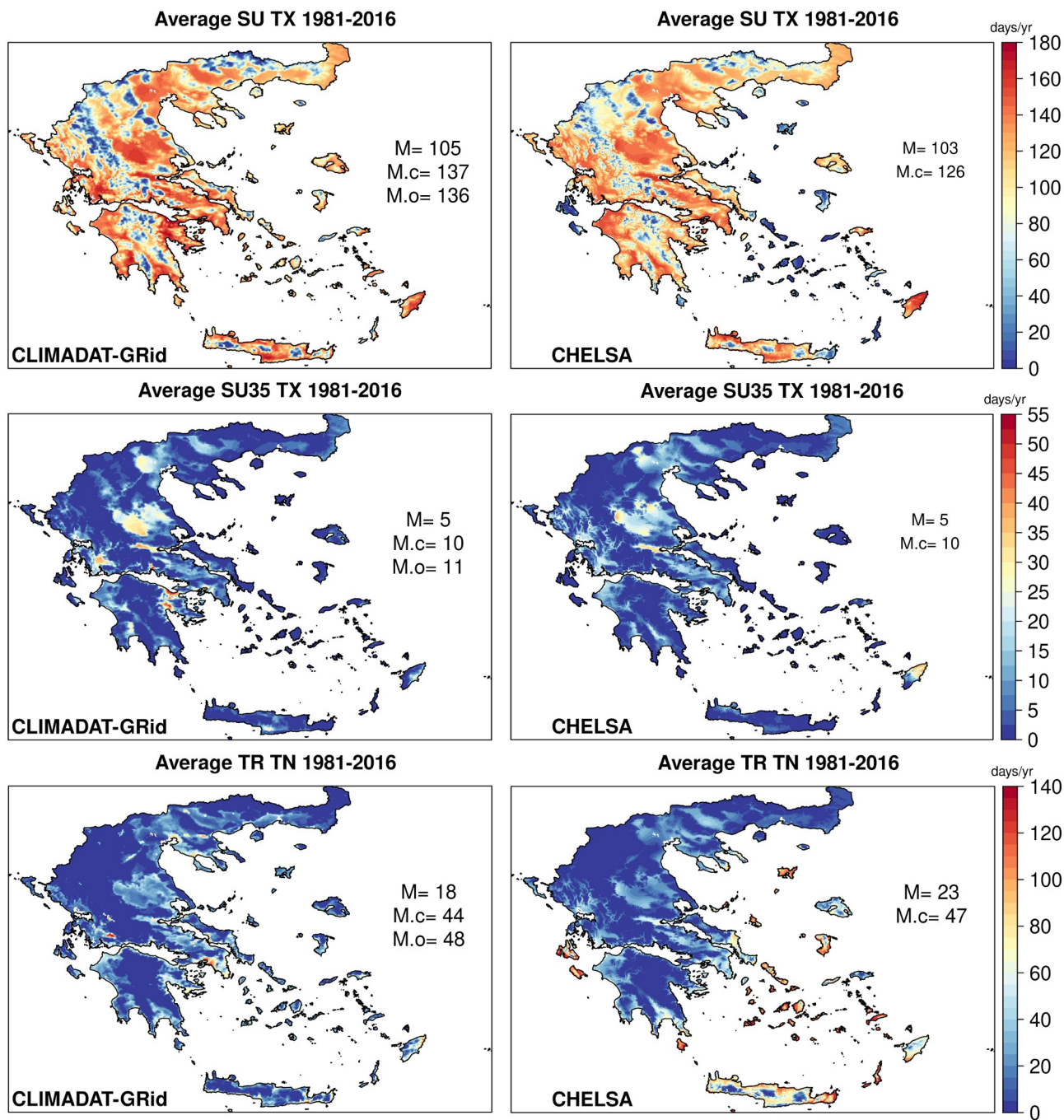


points covering the area whereas M.o denotes the station mean values while M.c the mean values for the closest grid points to the stations locations. Units are the same as in the colorbar.





335 **Figure 9.** Average annual and seasonal *TN* (winter (DJF), spring (MAM), summer (JJA) and autumn (SON)) for the period 1981–
 2016 for CLIMADAT-GRid (left column) and CHELSA (right column). In each panel, *M* denotes the spatial average over the grid
 points covering the area whereas *M.o* denotes the station mean values while *M.c* the mean values for the closest grid points to the
 stations locations. Units are the same as in the colorbar.



340



Figure 10. Average annual number of days $TX > 25^{\circ}\text{C}$ (SU), number of days $TX > 35^{\circ}\text{C}$ (SU35) and number of days $TN > 20^{\circ}\text{C}$ (TR) for the period 1981–2016 for CLIMADAT-GRid (left column) and CHELSA (right column). In each panel, M denotes the spatial average over the grid points covering the area whereas M.o denotes the station mean values while M.c the mean values for the closest grid points to the stations locations. Units are the same as in the colorbar.

345 4.2.2 Precipitation results

Figure 11 presents the total annual and seasonal precipitation results averaged over the period 1981–2016 for both datasets. In general, CLIMADAT-GRid indicates higher precipitation values compared to CHELSA on both the annual and the seasonal timescales. Both datasets capture the west-to-east precipitation gradient in Greece, with wetter conditions prevailing in the west and drier conditions in the east. However, the differences are more pronounced in CLIMADAT-GRid,
 350 particularly during Greece's rainy seasons (SON and DJF). When compared to the observations CLIMADAT-GRid indicates negligible biases, while for CHELSA the relative biases are about 18 % for the annual total precipitation and for the seasonal precipitation the biases range from about 15 % in SON to about 24 % in JJA with the rest of the seasons indicating intermediate biases.

Regarding the number of wet days (RR1, Fig. 12) the results are different since both datasets indicate a clear overestimation
 355 compared to the observed spatial means, with CLIMADAT-GRid indicating a more pronounced orographic pattern than CHELSA. This highly positive bias in the number of wet days has also been found in other gridded products (e.g., IBERIA01) and it is a byproduct of the selected interpolation methods. One way to reduce the inflated number of wet days is to introduce a third term in the interpolation scheme of precipitation by interpolating the daily occurrence of rainfall (0 or 1 depending on whether $PR > 0.1$ mm) considering a threshold between 0.1 and 0.9 for assigning a wet day to a grid point
 360 (Cornes et. al., 2018; Varotsos et al., 2023a). For instance, if we assign a value of 0.2 for the wet days and multiply the interpolated fields with the daily precipitation product the average number of wet days is reduced to 90 days/year with however increased underestimation in the annual and seasonal precipitation sums (not shown). For future studies utilizing the CLIMADAT-GRid precipitation dataset, a threshold of 2 mm/day could be considered when analyzing the number of wet days.

365 Finally, for the number of days with precipitation amounts higher or equal than 10 mm (R10mm, Fig. 12) both datasets exhibit similar results as it is shown from the spatial means with CLIMADAT-GRid indicating higher values for the specific index than CHELSA and closer to the observed spatial means. The highest values are shown for both datasets in western Greece, while the lowest in the eastern areas of the Greek domain.

370



375

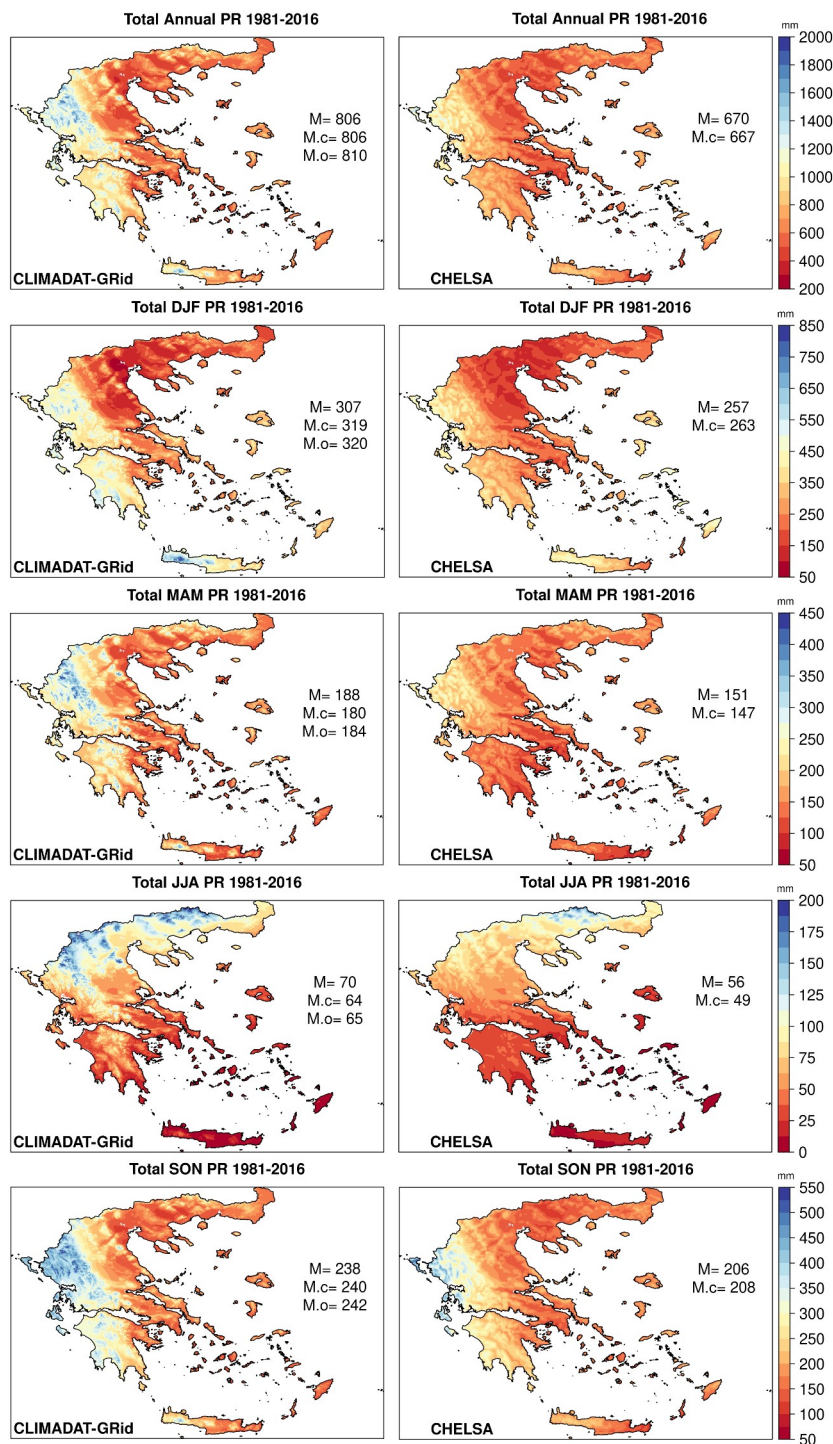
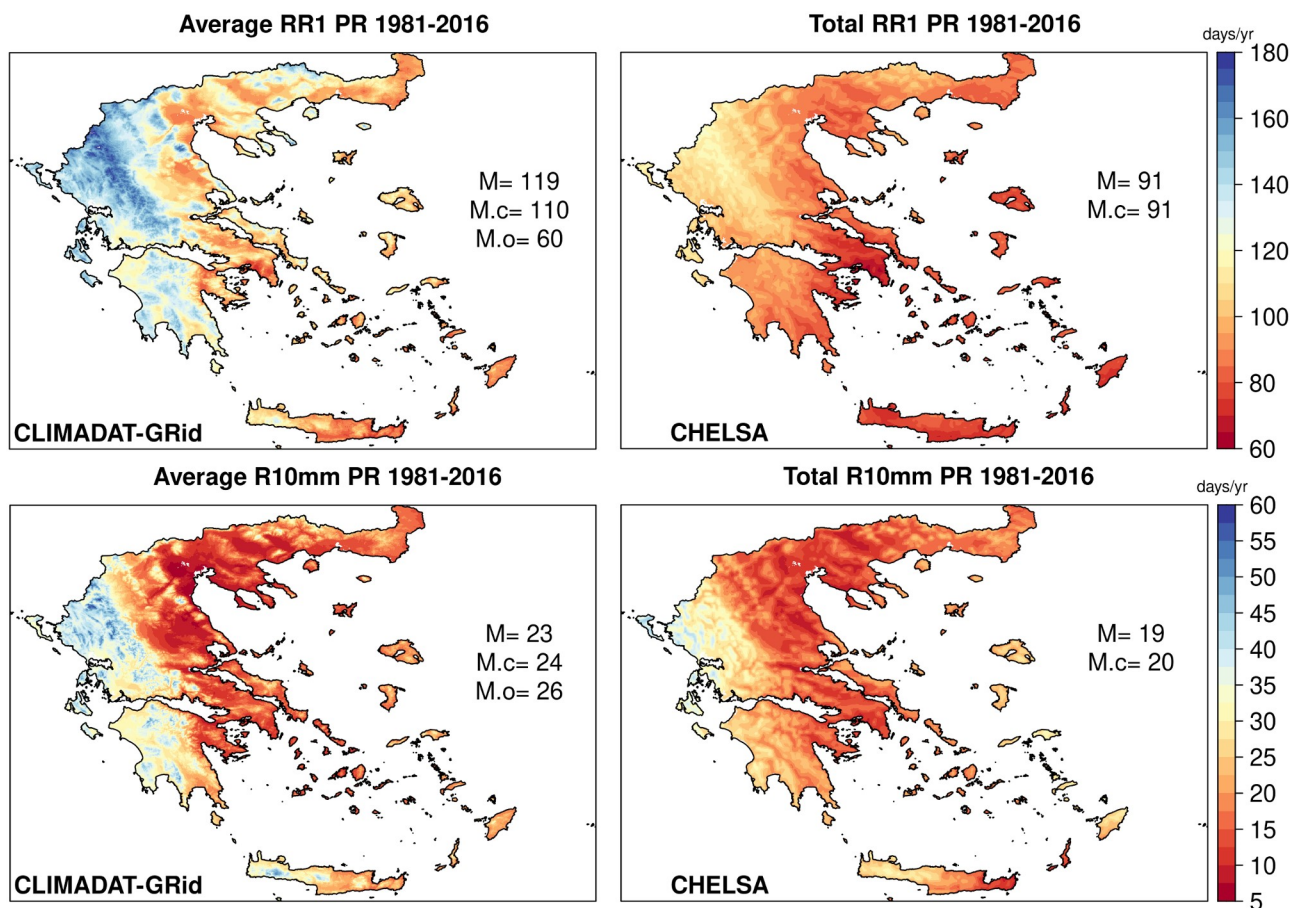


Figure 11. Total annual and seasonal PR (winter (DJF), spring (MAM), summer (JJA) and autumn (SON)) for the period 1981–2016 for CLIMADAT-GRid (left column) and CHELSA (right column). In each panel, M denotes the spatial average over the grid



380 points covering the area whereas M.o denotes the station mean values while M.c the mean values for the closest grid points to the stations locations. Units are the same as in the colorbar.



385 Figure 12. Average annual number of days $PR > 1$ mm (RR1) and number of days $PR \geq 10$ mm (R10mm) for the period 1981–2016 for CLIMADAT-GRid (left column) and CHELSA (right column). In each panel, M denotes the spatial average over the grid points covering the area whereas M.o denotes the station mean values while M.c the mean values for the closest grid points to the stations locations. Units are the same as in the colorbar.

5 Data availability

The CLIMADAT-GRid dataset is freely available in the web repository Zenodo (<https://doi.org/10.5281/zenodo.14637536>) and cited as Varotsos et al. (2025). Moreover the dataset is available through
 390 http://ostralia.meteo.noa.gr/repo/CLIMADAT_Grid/ (last access 19-12-2024). The NOAA network measurements and the historical weather station data from the National Observatory of Athens in Thessio are available via the CLIMPACT data repository
<https://data.climpact.gr/en/dataset/497dc26d-45e0-4ad5-b8f3-5f8890f65129> and
<https://data.climpact.gr/en/dataset/2f5bbe2a-7e27-40e7-9ff6-1dcc08c507fa>, respectively (last access 20-3-2024). ERA5-land



were obtained from the Copernicus Climate Data Store (last access 17-4-2024) while CHELSA-W5 were obtained from
395 <https://data.isimip.org/10.48364/ISIMIP.836809.2> (last access 17-07-2024).

6 Conclusions

In this paper, we described the construction of CLIMADAT-GRid, a new publicly available 1 km x 1 km daily gridded
climate dataset for Greece that focuses on temperatures and precipitation from 1981 to 2019. CLIMADAT-GRid is based on
400 quality-controlled and homogenized daily temperature and precipitation data gathered from 122 and 312 stations,
respectively. For the construction of the daily gridded datasets, various methods were examined whose accuracy was
assessed against withheld data. In addition, to obtain the gridded temperature data the observations were blended with a high
resolution WRF simulation over Greece for the year 1999.

The comparison with the CHELSA-W5E5 dataset for the period 1981–2016 showed that CLIMADAT-GRid generally
405 produced similar results for temperatures but captured spatial variability better with a closer agreement to observations on
both the mean values and the extremes. For *TX*, both datasets showed similar temperatures, with CLIMADAT-GRid closely
matching station data, while CHELSA consistently underestimating the observations by 0.5 to 0.7 °C. CLIMADAT-GRid
also better captured the temperature gradients in mountainous areas compared to CHELSA. Conversely, for *TN*, both
datasets showed identical spatial means overall, with a tendency in CHELSA to overestimate observations. The differences
410 between the datasets were most noticeable in the Ionian Sea islands, Crete, and the Aegean Sea islands, with CHELSA
showing higher temperatures in these regions. Regarding the extremes, both datasets produced similar spatial means for the
number of days with maximum temperatures above 25 °C and 35 °C, with CLIMADAT-GRid indicating the lowest biases
compared to the observations. However, CHELSA indicated a higher number of days with minimum temperatures above 20
°C compared to CLIMADAT-GRid. The spatial variability of these results is most noticeable in the Ionian and Aegean
415 islands, with CLIMADAT-GRid effectively capturing hotspots. Overall, the study highlights the differences between
CLIMADAT-GRid and CHELSA in capturing temperature variations in different regions, with CHELSA often
underestimating or overestimating observations compared to CLIMADAT-GRid.

For precipitation, the comparison between CLIMADAT-GRid and CHELSA datasets for the annual and seasonal
precipitation in Greece during the period 1981–2016 revealed that CLIMADAT-GRid generally indicated higher
420 precipitation values compared to CHELSA. Both datasets capture the west-to-east gradient of precipitation in Greece, with
the differences being more pronounced in CLIMADAT-GRid, especially during the rainy season. When compared to
observations, CLIMADAT-GRid had negligible biases, while CHELSA indicated relatively high biases ranging from 15-24
% depending on the season. Concerning the number of wet days, both datasets overestimate compared to observed spatial
means, with CLIMADAT-GRid showing a more pronounced orographic pattern than CHELSA. Moreover, both datasets



425 show similar results in the number of days with precipitation amounts equal to or higher than 10 mm, with CLIMADAT-GRid indicating higher values for this specific index in western Greece and better agreement with the observations. In conclusion, CLIMADAT-GRid serves as a valuable resource for climate research in Greece, providing high-resolution daily gridded datasets for temperatures and precipitation. Future work involves the construction of gridded datasets for other variables, such as relative humidity and wind speed, as well as extending the dataset to include more recent years.

430 **Author contribution**

KVV and CG conceptualized this study, GiKi, AK, IL, AS collected and provided the observational data, GeKa, VT, BP performed the quality control of the observational data, PP and MH performed the WRF simulations, KVV homogenized the observational data, implemented the code to perform the interpolation and the analysis and created the dataset and figures of the paper; KVV designed and wrote the manuscript with contribution from CG, GeKa, AGK, MGG, AK and GiKi; all
435 authors have read and approved the manuscript; financial support CG.

Competing interests

The authors declare that they have no conflict of interest.

Acknowledgements

The authors are grateful to the data providers of the Automatic Network and the Historical Weather Station of the National
440 Observatory of Athens, the Hellenic National Meteorological Service and the General Secretariat for Natural Environment and Water of the Ministry of Environment and Energy.

Financial support

This study is part of the “High resolution gridded CLIMate change DATasets for Greece, CLIMADAT-hub” project (<https://www.climadathub.gr/>). This project is carried out within the framework of the National Recovery and Resilience
445 Plan Greece 2.0, funded by the European Union – NextGenerationEU (Implementation body: HFRI, Project ID: 15478)

References

Avila-Diaz, A., Bromwich, D. H., Wilson, A. B., Justino, F., and Wang, S.-H.: Climate extremes across the North American Arctic in modern reanalyses, *Journal of Climate*, 34, 2385–2410, <https://doi.org/10.1175/JCLI-D-20-0093.1>, 2021.



- Beck, H. E., Pan, M., Roy, T., Weedon, G. P., Pappenberger, F., Van Dijk, A. I. J. M., Huffman, G. J., Adler, R. F., and
 450 Wood, E. F.: Daily evaluation of 26 precipitation datasets using Stage-IV gauge-radar data for the CONUS, *Hydrology and
 Earth System Sciences*, 23, 207–224, <https://doi.org/10.5194/hess-23-207-2019>, 2019.
- Beguiría, S., Vicente Serrano, S. M., Tomás-Burguera, M., and Maneta, M.: Bias in the variance of gridded data sets leads to
 misleading conclusions about changes in climate variability, *International Journal of Climatology*, 36, 3413–3422,
<https://doi.org/10.1002/joc.4561>, 2016.
- 455 Bhuiyan, M. A. E., Nikolopoulos, E. I., and Anagnostou, E. N.: Machine learning–based blending of satellite and reanalysis
 precipitation datasets: A multiregional tropical complex terrain evaluation, *Journal of Hydrometeorology*, 20, 2147–2161,
<https://doi.org/10.1175/JHM-D-19-0073.1>, 2019.
- Bonsoms, J., and Ninyerola, M.: Comparison of linear, generalized additive models and machine learning algorithms for
 spatial climate interpolation, *Theoretical and Applied Climatology*, 155, 1777–1792, [https://doi.org/10.1007/s00704-023-
 04725-5](https://doi.org/10.1007/s00704-023-

 460 04725-5), 2024.
- Cornes, R. C., van der Schrier, G., van den Besselaar, E. J. M., and Jones, P. D.: An ensemble version of the E-OBS
 temperature and precipitation data sets, *Journal of Geophysical Research: Atmospheres*, 123, 9391–9409,
<https://doi.org/10.1029/2017JD028200>, 2018.
- Déqué, M.: Frequency of precipitation and temperature extremes over France in an anthropogenic scenario: Model results
 465 and statistical correction according to observed values, *Global and Planetary Change*, 57, 16–26,
<https://doi.org/10.1016/j.gloplacha.2006.11.030>, 2007.
- Gofa, F., Mamara, A., Anadranistakis, M., and Flocas, H.: Developing gridded climate data sets of precipitation for Greece
 based on homogenized time series, *Climate*, 7, 68, <https://doi.org/10.3390/cli7050068>, 2019.
- Guijarro, J. A.: User’s guide of the climatol R Package (version 4.1. 1), 2023.
- 470 Haylock, M. R., Hofstra, N., Klein Tank, A. M. G., Klok, E. J., Jones, P. D., and New, M.: A European daily high-resolution
 gridded data set of surface temperature and precipitation for 1950–2006, *Journal of Geophysical Research: Atmospheres*,
 113, <https://doi.org/10.1029/2008JD010201>, 2008.
- Hernanz, A., Correa, C., Sánchez-Perrino, J.-C., Prieto-Rico, I., Rodríguez-Guisado, E., Domínguez, M., and Rodríguez-
 Camino, E.: On the limitations of deep learning for statistical downscaling of climate change projections: The transferability
 475 and the extrapolation issues, *Atmospheric Science Letters*, 25, e1195, <https://doi.org/10.1002/asl.1195>, 2024.
- Herrera, S., Gutiérrez, J. M., Ancell, R., Pons, M. R., Frías, M. D., and Fernández, J.: Development and analysis of a 50-year
 high-resolution daily gridded precipitation dataset over Spain (Spain02), 2012.
- Herrera, S., Cardoso, R. M., Soares, P. M., Espírito-Santo, F., Viterbo, P., and Gutiérrez, J. M.: Iberia01: A new gridded
 dataset of daily precipitation and temperatures over Iberia, *Earth System Science Data*, 11, 1947–1956,
 480 <https://doi.org/10.5194/essd-11-1947-2019>, 2019.



- Hersbach, H., Bell, B., Berrisford, P., Hirahara, S., Horányi, A., Muñoz-Sabater, J. n., Nicolas, J., Peubey, C., Radu, R., Schepers, D., and others: The ERA5 global reanalysis, *Quarterly Journal of the Royal Meteorological Society*, 146, 1999–2049, <https://doi.org/10.1002/qj.3803>, 2020.
- Hofstra, N., New, M., and McSweeney, C.: The influence of interpolation and station network density on the distributions and trends of climate variables in gridded daily data, *Climate dynamics*, 35, 841–858, <https://doi.org/10.1007/s00382-009-0698-1>, 2010.
- Hong, S.-Y., Noh, Y., and Dudhia, J.: A new vertical diffusion package with an explicit treatment of entrainment processes, *Monthly weather review*, 134, 2318–2341, <https://doi.org/10.1175/MWR3199.1>, 2006.
- Hu, W., Scholz, Y., Yeligeti, M., von Bremen, L., and Deng, Y.: Downscaling ERA5 wind speed data: a machine learning approach considering topographic influences, *Environmental Research Letters*, 18, 094007, <https://doi.org/10.1088/1748-9326/aceb0a>, 2023.
- Hutchinson, M. F., McKenney, D. W., Lawrence, K., Pedlar, J. H., Hopkinson, R. F., Milewska, E., and Papadopol, P.: Development and testing of Canada-wide interpolated spatial models of daily minimum–maximum temperature and precipitation for 1961–2003, *Journal of Applied Meteorology and Climatology*, 48, 725–741, <https://doi.org/10.1175/2008JAMC1979.1>, 2009.
- Iacono, M. J., Delamere, J. S., Mlawer, E. J., Shephard, M. W., Clough, S. A., and Collins, W. D.: Radiative forcing by long-lived greenhouse gases: Calculations with the AER radiative transfer models, *Journal of Geophysical Research: Atmospheres*, 113, <https://doi.org/10.1029/2008JD009944>, 2008.
- Johnson, M. E., Moore, L. M., and Ylvisaker, D.: Minimax and maximin distance designs, *Journal of statistical planning and inference*, 26, 131–148, [https://doi.org/10.1016/0378-3758\(90\)90122-B](https://doi.org/10.1016/0378-3758(90)90122-B), 1990.
- Kain, J. S.: The Kain–Fritsch convective parameterization: an update, *Journal of applied meteorology*, 43, 170–181, [https://doi.org/10.1175/1520-0450\(2004\)043<0170:TKCPAU>2.0.CO;2](https://doi.org/10.1175/1520-0450(2004)043<0170:TKCPAU>2.0.CO;2), 2004.
- Karali, A., Varotsos, K. V., Giannakopoulos, C., Nastos, P. P., and Hatzaki, M.: Seasonal fire danger forecasts for supporting fire prevention management in an eastern Mediterranean environment: The case of Attica, Greece, *Natural hazards and earth system sciences*, 23, 429–445, <https://doi.org/10.5194/nhess-23-429-2023>, 2023.
- Karger, D. N., Lange, S., Hari, C., Reyer, C. P. O., Conrad, O., Zimmermann, N. E., and Frieler, K.: CHELSA-W5E5: Daily 1 km meteorological forcing data for climate impact studies, *Earth System Science Data*, 15, 2445–2464, <https://doi.org/10.5194/essd-15-2445-2023>, 2023.
- Kuhn, M.: Building predictive models in R using the caret package, *Journal of statistical software*, 28, 1–26, <https://doi.org/10.18637/jss.v028.i05>, 2008.
- Lagouvardos, K., Kotroni, V., Bezes, A., Koletsis, I., Kopania, T., Lykoudis, S., Mazarakis, N., Papagiannaki, K., and Vougioukas, S.: The automatic weather stations NOANN network of the National Observatory of Athens: Operation and database, *Geoscience Data Journal*, 4, 4–16, <https://doi.org/10.1002/gdj3.44>, 2017.



- Lorenz, C., Portele, T. C., Laux, P., and Kunstmann, H.: Bias-corrected and spatially disaggregated seasonal forecasts: a
 515 long-term reference forecast product for the water sector in semi-arid regions, *Earth System Science Data*, 13, 2701–2722,
<https://doi.org/10.5194/essd-13-2701-2021>, 2021.
- Lussana, C., Saloranta, T., Skaugen, T., Magnusson, J., Tveito, O. E., and Andersen, J.: seNorge2 daily precipitation, an
 observational gridded dataset over Norway from 1957 to the present day, *Earth System Science Data*, 10, 235–249,
<https://doi.org/10.5194/essd-10-235-2018>, 2018a.
- 520 Lussana, C., Tveito, O. E., and Uboldi, F.: Three-dimensional spatial interpolation of 2 m temperature over Norway,
Quarterly Journal of the Royal Meteorological Society, 144, 344–364, <https://doi.org/10.1002/qj.3208>, 2018b.
- Mamara, A., Anadranistakis, M., Argiriou, A. A., Szentimrey, T., Kovacs, T., Bezes, A., and Bihari, Z.: High resolution air
 temperature climatology for Greece for the period 1971–2000, *Meteorological Applications*, 24, 191–205,
<https://doi.org/10.1002/met.1617>, 2017.
- 525 Muñoz-Sabater, J. n., Dutra, E., Agustí-Panareda, A., Albergel, C., Arduini, G., Balsamo, G., Boussetta, S., Choulga, M.,
 Harrigan, S., Hersbach, H., and others: ERA5-Land: A state-of-the-art global reanalysis dataset for land applications, *Earth
 system science data*, 13, 4349–4383, <https://doi.org/10.5194/essd-13-4349-2021>, 2021.
- Nilsen, I. B., Hanssen-Bauer, I., Dyrørdal, A. V., Hisdal, H., Lawrence, D., Haddeland, I., and Wong, W. K.: From climate
 model output to actionable climate information in Norway, *Frontiers in Climate*, 4, 866563,
 530 <https://doi.org/10.3389/fclim.2022.866563>, 2022.
- Nwaila, G. T., Zhang, S. E., Bourdeau, J. E., Frimmel, H. E., and Ghorbani, Y.: Spatial interpolation using machine learning:
 from patterns and regularities to block models, *Natural Resources Research*, 33, 129–161, [https://doi.org/10.1007/s11053-
 023-10280-7](https://doi.org/10.1007/s11053-023-10280-7), 2024.
- Nychka, D., Bandyopadhyay, S., Hammerling, D., Lindgren, F., and Sain, S.: A multiresolution Gaussian process model for
 535 the analysis of large spatial datasets, *Journal of Computational and Graphical Statistics*, 24, 579–599,
<https://doi.org/10.1080/10618600.2014.914946>, 2015.
- Nychka, D., Furrer, R., Paige, J., Sain, S., and Nychka, M. D.: Package ‘fields’, URL
<http://cran.r-project.org/web/packages/fields/fields.pdf>, 2015.
- Nychka, D., Hammerling, D., Sain, S., Lenssen, N., and Nychka, M. D.: Package ‘LatticeKrig’, 2019.
- 540 Otero-Casal, C., Patlakas, P., Prósper, M. A., Galanis, G., and Miguez-Macho, G.: Development of a high-resolution wind
 forecast system based on the WRF model and a hybrid Kalman-Bayesian filter, *Energies*, 12, 3050,
<https://doi.org/10.3390/en12163050>, 2019.
- Papa, K.M., and Koutroulis, A.G.: Evaluation of precipitation datasets over Greece. Insights from comparing multiple
 gridded products with observations, *Atmospheric Research*, 315, 107888, <https://doi.org/10.1016/j.atmosres.2024.107888>,
 545 2025.
- Patlakas, P., Stathopoulos, C., Kalogeri, C., Vervatis, V., Karagiorgos, J., Chaniotis, I., Kallos, A., Ghulam, A. S., Al-omary,
 M. A., Papageorgiou, I., and others: The Development and Operational Use of an Integrated Numerical Weather Prediction



- System in the National Center for Meteorology of the Kingdom of Saudi Arabia, Weather and Forecasting, 38, 2289–2319, <https://doi.org/10.1175/WAF-D-23-0034.1>, 2023.
- 550 Powers, J. G., Klemp, J. B., Skamarock, W. C., Davis, C. A., Dudhia, J., Gill, D. O., Coen, J. L., Gochis, D. J., Ahmadov, R., Peckham, S. E., and others: The weather research and forecasting model: Overview, system efforts, and future directions, *Bulletin of the American Meteorological Society*, 98, 1717–1737, <https://doi.org/10.1175/BAMS-D-15-00308.1>, 2017.
- Qin, R., Zhao, Z., Xu, J., Ye, J.-S., Li, F.-M., and Zhang, F.: HRLT: a high-resolution (1 d, 1 km) and long-term (1961–2019) gridded dataset for surface temperature and precipitation across China, *Earth System Science Data*, 14, 4793–4810, <https://doi.org/10.5194/essd-14-4793-2022>, 2022.
- 555 R core team: The R Project for Statistical Computing, <https://www.r-project.org/>, 2024.
- Sekulić, A., Kilibarda, M., Protić, D., and Bajat, B.: A high-resolution daily gridded meteorological dataset for Serbia made by Random Forest Spatial Interpolation, *Scientific Data*, 8, 123, <https://doi.org/10.1038/s41597-021-00901-2>, 2021.
- Skamarock, W. C.: A description of the advanced research WRF version 3, NCAR/TN–475+STR NCAR TECHNICAL
 560 NOTE, 125, 2008.
- Skamarock, W. C., Klemp, J. B., Dudhia, J., Gill, D. O., Liu, Z., Berner, J., Wang, W., Powers, J. G., Duda, M. G., Barker, D. M., and others: A description of the advanced research WRF version 4, NCAR tech. note ncar/tn-556+ str, 145, 2019.
- Slater, J. A., Heady, B., Kroenung, G., Curtis, W., Haase, J., Hoegemann, D., Shockley, C., and Tracy, K.: Global assessment of the new ASTER global digital elevation model, *Photogrammetric Engineering & Remote Sensing*, 77, 335–
 565 349, <https://doi.org/10.14358/PERS.77.4.335>, 2011.
- Sofia, G., Yang, Q., Shen, X., Mitu, M. F., Patlakas, P., Chaniotis, I., Kallos, A., Alomary, M. A., Alzahrani, S. S., Christidis, Z., and others: A Nationwide Flood Forecasting System for Saudi Arabia: Insights from the Jeddah 2022 Event, *Water*, 16, 1939, <https://doi.org/10.3390/w16141939>, 2024.
- Stathopoulos, C., Chaniotis, I., and Patlakas, P.: Assimilating Aeolus Satellite Wind Data on a Regional Level: Application
 570 in a Mediterranean Cyclone Using the WRF Model, *Atmosphere*, 14, 1811, <https://doi.org/10.3390/atmos14121811>, 2023.
- Thompson, G., Rasmussen, R. M., and Manning, K.: Explicit forecasts of winter precipitation using an improved bulk microphysics scheme. Part I: Description and sensitivity analysis, *Monthly Weather Review*, 132, 519–542, [https://doi.org/10.1175/1520-0493\(2004\)132<0519:EFOWPU>2.0.CO;2](https://doi.org/10.1175/1520-0493(2004)132<0519:EFOWPU>2.0.CO;2), 2004.
- Tveito, O. E., Førland, E. J., Heino, R., Hanssen-Bauer, I., Alexandersson, H., Dahlström, B., Drebs, A., Kern-Hansen, C.,
 575 Jónsson, T., Vaarby-Laursen, E., and others: Nordic Temperature Maps, DNMI Klima 9/00 KLIMA, Oslo, Norway: Norwegian Meteorological Institute, 2000.
- Tveito, O. E., Bjørdal, I., Skjelvåg, A. O., and Aune, B.: A GIS-based agro-ecological decision system based on gridded climatology, *Meteorological Applications*, 12, 57–68, <https://doi.org/10.1017/S1350482705001490>, 2005.
- Varotsos, K. V., Dandou, A., Papangelis, G., Roukounakis, N., Kitsara, G., Tombrou, M., and Giannakopoulos, C.: Using a
 580 new local high resolution daily gridded dataset for Attica to statistically downscale climate projections, *Climate Dynamics*, 60, 2931–2956, <https://doi.org/10.1007/s00382-022-06482-z>, 2023a.



- Varotsos, K. V., Katavoutas, G., and Giannakopoulos, C.: On the Use of Reanalysis Data to Reconstruct Missing Observed Daily Temperatures in Europe over a Lengthy Period of Time, *Sustainability*, 15, 7081, <https://doi.org/10.3390/su15097081>, 2023b.
- 585 Varotsos, K. V., Kitsara, G., Karali, A., Lemesios, I., Patlakas, P., Hatzaki, M., Tenentes, V., Katavoutas, G., Sarantopoulos, A., Psiloglou, B., Koutroulis, A. G., Grillakis, M. G., and Giannakopoulos, C.: CLIMADAT-GRid: A high-resolution (1 km x 1 km) daily gridded precipitation and temperature dataset for Greece, Zenodo, Version 1, <https://doi.org/10.5281/zenodo.14637536>, 2025.
- Wood, S., and Wood, M. S.: Package ‘mgcv’, R package version, 1, 729, 2015.
- 590 Wood, S. N.: Generalized additive models: an introduction with R, Chapman and Hall/CRC, 2017.
- Zhang, X., Alexander, L., Hegerl, G. C., Jones, P., Tank, A. K., Peterson, T. C., Trewin, B., and Zwiers, F. W.: Indices for monitoring changes in extremes based on daily temperature and precipitation data, *Wiley Interdisciplinary Reviews: Climate Change*, 2, 851–870, <https://doi.org/10.1002/wcc.147>, 2011.